

Article

The Relationship between Roadside PM Concentration and Traffic Characterization: A Case Study in Macao

Thomas M. T. Lei  and Martin F. C. Ma 

Institute of Science and Environment, University of Saint Joseph, Macao, China

* Correspondence: thomas.lei@usj.edu.mo

Abstract: Road transportation is a common mode of transport in Macao and is also known to be a significant source of the emission of PM₁₀ and PM_{2.5} on a local and regional scale. There are six air quality monitoring stations (AQMS) evenly distributed throughout Macao, but some densely populated areas are currently not covered by the monitoring network. Therefore, a monitoring campaign was conducted at four roadside locations in Macao's most densely populated areas. This work aims to study the concentrations of PM₁₀ and PM_{2.5} in several roadside locations in Macao. The monitoring campaign was conducted for 24 non-consecutive periods, with a total of 192 monitoring hours. The sampling sites were chosen based on Macao's most densely populated areas and the most traffic-congested locations. In addition, traffic characterization was performed alongside the monitoring campaign to provide a clearer perspective on the pollution sources. Based on the collected data, a correlation analysis was performed between the number of vehicles and the levels of PM₁₀ and PM_{2.5} concentration. The results showed a weak relationship between the hourly traffic flow and the level of PM₁₀ and PM_{2.5} concentrations, with a correlation of determination (R^2) of 0.001 to 0.122. In addition, the results showed a weak relationship between the vehicle types and the level of PM₁₀ and PM_{2.5} concentrations, with an R^2 of 0.000 to 0.043. As shown, there is little to no relationship between local traffic volume and roadside PM concentration in the monitored locations of Macao, leading us to conclude that PM concentration is more likely tied to regional sources and meteorological conditions. Nevertheless, the complex geographical setting of Macao is also likely an influential factor in this study.

Keywords: air quality; air pollution; particulate matter; monitoring campaign; traffic characterization



Citation: Lei, T.M.T.; Ma, M.F.C. The Relationship between Roadside PM Concentration and Traffic Characterization: A Case Study in Macao. *Sustainability* **2023**, *15*, 10993. <https://doi.org/10.3390/su151410993>

Academic Editors: Sarkawt Hama, Giovanni Gualtieri, Ülkü Alver Şahin and Yetkin Dumanoglu

Received: 10 May 2023

Revised: 7 July 2023

Accepted: 10 July 2023

Published: 13 July 2023



Copyright: © 2023 by the authors. Licensee MDPI, Basel, Switzerland. This article is an open access article distributed under the terms and conditions of the Creative Commons Attribution (CC BY) license (<https://creativecommons.org/licenses/by/4.0/>).

1. Introduction

Road transportation is a common mode of transport in Macao due to the increasing convenience of motor vehicles. Private cars are used to avoid adverse weather conditions during the summer and winter seasons, which is also a known source of urban air pollution. Studies have found that air pollution kills more than 7 million people worldwide every year, with 4.2 million dying from outdoor air pollution and 3.8 million dying from indoor air pollution. In particular, fatalities result from pneumonia (21%), stroke (20%), ischemic heart disease (34%), chronic obstructive pulmonary disease (COPD) (19%), and lung cancer (7%). There are over 2 million people affected by air pollution in Southeast Asia [1–3].

A study in Macao identified an episode of high pollution during a week of the Chinese National Holiday of 2019 (1 to 7 October), in which high concentration levels were identified for PM_{2.5} and O₃, with a peak of daily levels reaching 55 µg/m³ and 400 µg/m³, respectively. In contrast, a low pollution episode for PM_{2.5} and O₃ was identified during the COVID-19 pandemic period, with a record low of daily levels of concentration for PM_{2.5} and O₃ registered at only 2 µg/m³ and 50 µg/m³, respectively [4]. These pollution episodes are caused by transboundary pollutants causing a regional problem in the Greater Bay Area, not limited to the region of Macao. Another study in Macao shows that the local emissions contributed to at least 35% of PM_{2.5} concentrations, and higher black carbon

(BC) concentrations were observed during the day than at night, which is consistent with the diurnal variations of traffic flow [5]. BC is the product of incomplete combustion that is mainly derived from diesel engines and rich-burned gasoline carburetor engines on scooters and light-duty vehicles [6].

Traffic-related emissions are a significant component of airborne pollution, and the measurement and analysis of real-world vehicle emissions have been used due to the fact that conventional drive cycle testing is not considered representative of vehicles under real-world driving conditions [7]. A study in South Korea shows that $PM_{2.5}$ emissions decreased by 0.6 to 4.1% under the subsidy policy for zero emission vehicles (ZEVs), including electric battery vehicles (BEVs) and fuel cell electric vehicles (FCEVs) for cars, buses, motorcycles, and freight trucks, but it did not reduce diesel freight trucks, which is a major contributor to $PM_{2.5}$ and NO_x [8]. The overall average of $PM_{2.5}$ mass is slightly higher than those measured in the urban site [9].

Vehicle emissions are among the major sources of airborne $PM_{2.5}$ in urban environments, which adversely impacts the environment and public health [10]. Vehicular emissions are a major source of carbonaceous aerosols at a heavily trafficked sampling site in Hong Kong [11]. Traffic is a major source of urban air pollution in developing countries, with $PM_{2.5}$ and BC being the primary sources of pollutants at the roadside [12]. The cause of roadside air pollution is due to a large number of on-road vehicles and traffic jams [13]. The contribution of roadway sources is about 12 to 17% of $PM_{2.5}$ at the near-road site [14]. The characterization of freshly emitted traffic aerosols in Hong Kong observed high levels of $PM_{2.5}$, OC, and EC at the roadside location [15]. The concentrations of CO and NO_2 were correlated with similar diurnal variations, with meteorological factors driving the diurnal variability more than traffic counts [16]. The concentration of indoor $PM_{2.5}$ was higher than that of outdoor $PM_{2.5}$ [17].

The monitoring of air pollution primarily relies on expensive, high-end static sensor stations, which only produce aggregated information about air pollutants but cannot capture the variations in an individuals' air pollution exposure [18]. The average hourly $PM_{2.5}$ concentration at a roadside location is approximately twice the concentration at nearby air quality monitoring station (AQMS) [19]. A monitoring campaign in Kenya successfully applied calibrated low-cost sensors to investigate the concentration of PM_{10} , $PM_{2.5}$, and PM_1 in the urban background and roadside locations [20]. A study in Yangon also successfully assessed the regional distribution of $PM_{2.5}$ using a portable $PM_{2.5}$ sensor [21].

The main challenge of air quality management in most cities is meeting air quality limits in areas with high road traffic [22]. The assessment of the air quality in metropolitan areas is a major challenge due to the distribution of monitoring stations [23]. Analysis of $PM_{2.5}$ in Tehran reveals that a large fraction of the total mass of $PM_{2.5}$ is composed of BC, especially during cold seasons [6]. There is a dominant percentage of ultra-fine particle (UFP) deposition in the lungs which strengthens the need to incorporate UFP into the current AQI [24]. A monitoring campaign shows that UFP increases with an increase in the number of flights [25]. A study in Lisbon identified marine transportation as a significant source of UFP [26]. Another study in South Korea attempted to identify the influencing factors that affected the concentration of resuspended road dust, and the result shows that further studies are needed to reach a conclusion [27]. Due to the limited area in Macao, there are no heavy industries, and the largest industry is gaming and tourism.

Thus, monitoring urban roadside air pollution using portable and affordable solutions and better understanding the impact of traffic characteristics on air quality is extremely important to protect the health and well-being of the local community. This study will determine if traffic emissions contribute to the concentration of PMs in the monitored locations of Macao. This is a preliminary study of roadside PM emissions in the high-density roadside area in Macao, which is surrounded by many residential buildings and is very important to the well-being of the nearby residents. This study employed low-cost portable equipment, and pre-recorded footage was used for traffic counting and characterization.

2. Materials and Methods

2.1. Meteorological Factors

Figure 1 shows the air mass arriving in Macao (100 m in height) during the days of the monitoring campaign in Macao. The backward trajectory of air mass is extracted from the Hong Kong Observatory (HKO) and prepared using the HYSPLIT model of NOAA. It shows that the path of the air mass that arrived in Macao this spring is mainly from the north and the northeast, and a part of the air mass from the south affects Macao (Figure 1). When the air mass directly arrives at Macao from the north or the air mass lingers and moves relatively slowly near Macao, the concentration of PM is generally higher than that of the air mass when approaching Macao from the sea. The levels of PM₁₀ and PM_{2.5} concentrations are highly influenced by the seasonal monsoon and wind direction.

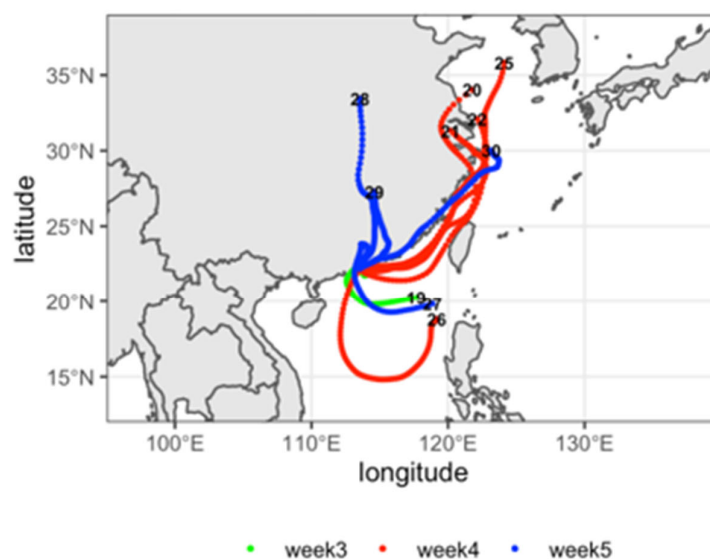


Figure 1. Past 72 h of backward trajectory of air mass reaching Macao (100 m height) on 15 March 2022.

Figure 2a presents the wind rose of Macao in hourly counts. The primary wind direction of Macao is coming from the north (N) and north-northeast (NNE), which may explain why particles such as PM₁₀ and PM_{2.5} could be transported by the wind from neighboring regions into Macao (Figure 2a).



Figure 2. (a) Wind level in Macao (hourly counts) (b) Wind speed (m/s) of Macao in the recent 5 years.

Figure 2b presents the wind speed (m/s) of Macao. The highest wind speed level comes from the north (N) and north-northeast (NNE) directions, with a mean wind speed of 4 m/s. The high wind speed level, predominantly coming from the northern quadrant, is likely to transport particles such as PM₁₀ and PM_{2.5} from neighboring regions into Macao at a high flow rate (Figure 2b).

Figure 3a presents the pollution level of PM₁₀ in Macao. The peak level of PM₁₀ concentration seemed to be arriving from the north-northeast (NNE) and northwest (NW) directions, with a mean concentration of 64 $\mu\text{g}/\text{m}^3$ and 65 $\mu\text{g}/\text{m}^3$, respectively (Figure 3a).

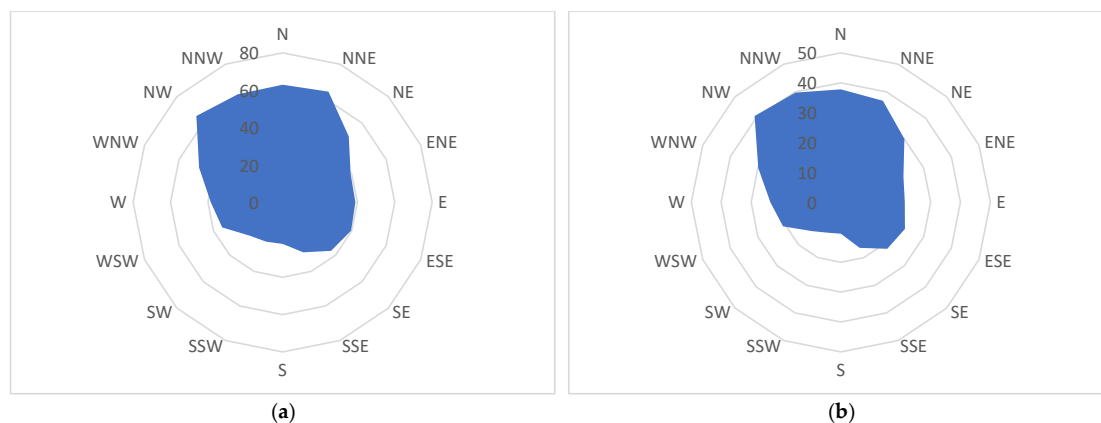


Figure 3. Pollution levels of (a) PM₁₀ ($\mu\text{g}/\text{m}^3$) and (b) PM_{2.5} ($\mu\text{g}/\text{m}^3$) in Macao in the recent 5 years.

Figure 3b presents the pollution rose of PM_{2.5} in Macao. The peak level of PM_{2.5} concentration seemed to be arriving from northwest (NW) and north-northwest (NNW) directions, with a mean concentration of 41 $\mu\text{g}/\text{m}^3$ and 40 $\mu\text{g}/\text{m}^3$, respectively (Figure 3b).

2.2. Study Area

According to previous studies, the levels of concentration for PM_{2.5} and O₃ in Macao often exceeded the levels recommended by the WHO AQG, and the Macao Meteorological and Geophysical Bureau (SMG) established six AQMS throughout the region of Macao, namely Macao Roadside, Macao High-Density Residential Area, Taipa Ambient, Taipa High-Density Residential Area, Coloane Ambient, and Ka-Ho Roadside [28]. The collection of PM data is difficult in a compact urban environment due to the limited roadside monitoring stations and complicated urban context, so a backpack outdoor environmental measuring unit can be used to monitor the PM in the most representative commercial districts [29]. In addition, mobile monitoring of air pollution is a growing field to fill in spatial gaps for personal air-quality-based risk assessment [30]. Figure 4a shows the six air quality monitoring stations' spatial location within the area of 32.8 km² in Macao, and Figure 4b shows the exact four roadside locations on a map where the monitoring campaign was conducted in this study (Figure 4a,b).

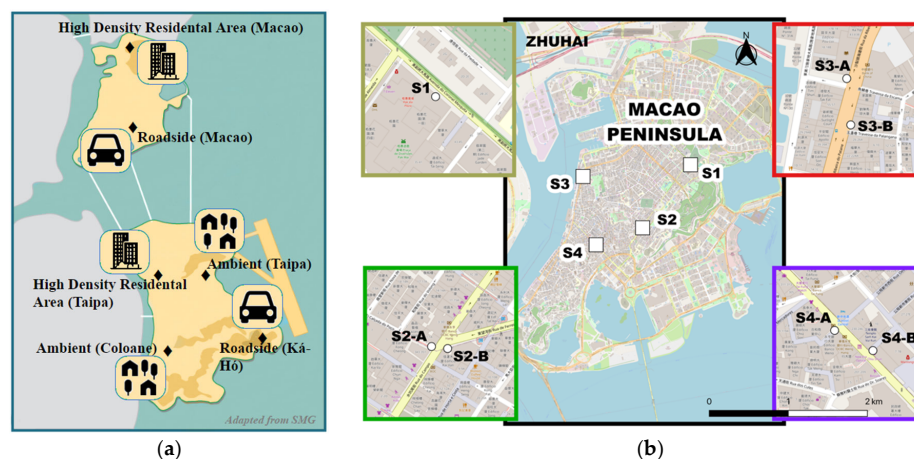


Figure 4. (a) Air quality monitoring network spatial location in Macao; (b) Different locations of conducted monitoring campaigns.

2.3. Monitoring Equipment

This monitoring campaign uses low-cost portable monitoring equipment, the TSI Sidepak AM510 Personal Aerosol Monitor, calibrated to the factory settings. This monitor is a portable and lightweight light-scattering laser photometer with a built-in sampling pump that provides a real-time mass concentration of PM. The portable equipment can provide real-time exposure compared to the fixed AQMS [21]. The meteorological parameters (wind speed (v), wind direction, temperature (T), and relative humidity (RH)) used in this study are obtained from the background ambient location of Taipa Ambient, the headquarters of the Macao Meteorological and Geophysical Bureau (SMG). The monitoring locations of the traffic-related sites included four sites in Macao, including Avenida do Coronel Mesquita (S1), Rua do Campo (S2-A and S2-B), Rua da Ribeira do Patane (S3-A and S3-B), and Avenida do Almeida Ribeiro (S4-A and S4-B), all of which are situated on the peninsula of Macao. These locations have a high population density and are not covered by the AQMS. The residential and commercial buildings are very close to the roadside, so the traffic emissions may pose potential health hazards to the residents.

2.4. Monitoring Period and Method

This intensive monitoring campaign was carried out in the four selected locations during the first half of 2022 (from March to May during the monsoon season). There are a combined twenty-four monitoring days for each location, with two hours of monitoring per session. The total monitoring hours of this campaign are 192 h. The traffic characteristics were conducted alongside the air quality monitoring campaign in all of the selected locations, with a vehicle count of 10 min in each direction (inbound and outbound) and extrapolated to an hour for each direction, with pre-recorded footage collected simultaneously with the roadside air quality monitoring. A total of 20 min of vehicle count were performed for each monitoring session. Traffic characterization by type of vehicle during sampling is categorized by the following: PC—passenger cars; LD—light-duty vehicles; T—taxi; B—buses; HD—heavy-duty vehicles; M—motorcycles.

2.5. Quality Control, Quality Assurance, and Calibration Factor (CF)

Although the TSI Sidepak AM510 Personal Aerosol Monitor is a simple and reliable instrument, it is important to establish quality control and quality assurance in the data collection. Therefore, the TSI Sidepak AM510 Personal Aerosol Monitor is placed next to the Met One BAM 1020 Continuous Particle Monitor, an US EPA equivalent method for PM₁₀ and PM_{2.5} monitoring. In this study, only field calibration of the TSI Sidepak Monitor was performed, as it is light-scattering equipment and could be affected by the humidity present in the air. The calibration results show a correlation coefficient (r) of 0.79 between the field calibrated equipment and the EPA equivalent reference method.

The calibration factor (CF) for PM₁₀ and PM_{2.5} derived from this study is 0.59 and 0.29, respectively. Figure 5a,b show the PM₁₀ measurement before and after QC/QA and calibration. Figure 5c,d show the PM_{2.5} measurement before and after QC/QA and calibration. As shown by Figure 5, there is a significant improvement in the accuracy of the measurement by the TSI Sidepak Monitor after calibration, which is very important for the result reported in this study (Figure 5a–d). Table 1 shows the performance indicator before and after the calibration. The RMSE and MAE after calibration have significantly improved, for PM₁₀, they are 12.03 and 9.07, respectively, and for PM_{2.5}, they are 5.76 and 4.47, respectively (see Table 1).

$$RMSE = \sqrt{\sum_{i=1}^n \left(y_{pred}^i - y_{true}^i \right)^2 * \frac{1}{n}} \quad (1)$$

$$MAE = \frac{1}{n} \sum_{i=1}^n \left| y_{pred}^i - y_{true}^i \right| \quad (2)$$

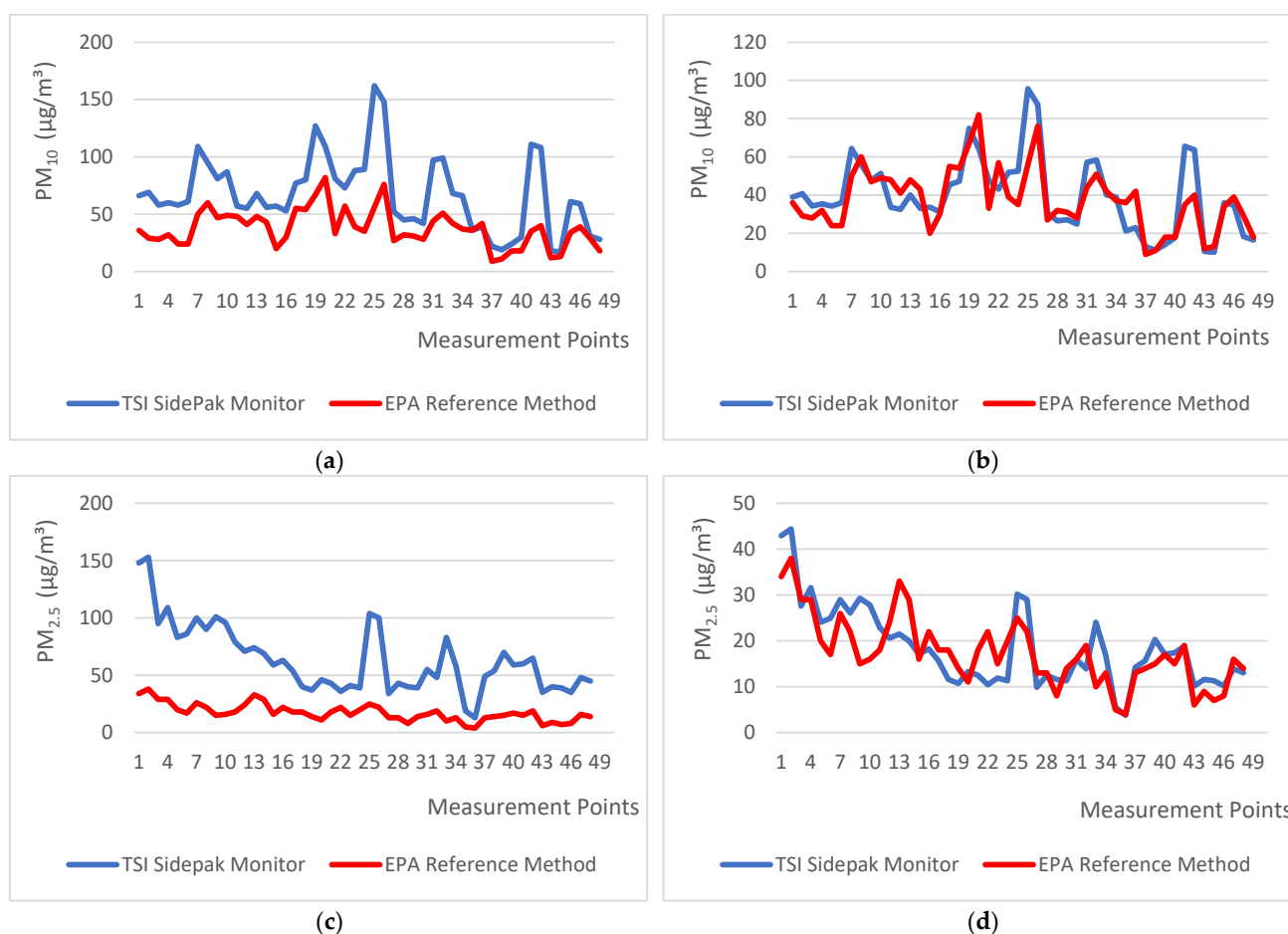


Figure 5. (a) PM_{10} measurement before QC/QA and calibration (b) PM_{10} measurement after QC/QA and calibration. (c) $PM_{2.5}$ measurement before QC/QA and calibration (d) $PM_{2.5}$ measurement after QC/QA and calibration.

Table 1. Performance indicator before and after calibration with EPA reference methods.

	PM_{10}	$PM_{2.5}$
RMSE Before Calibration	37.22	52.12
RMSE After Calibration	12.03	5.76
MAE Before Calibration	29.98	46.00
MAE After Calibration	9.07	4.47

3. Results and Discussion

According to the Macao Environmental Protection Bureau (DSPB), the major emission sources for various suspended particulates (TSP, PM_{10} , and $PM_{2.5}$) are from the construction and land transport sectors, accounting for about 40% and 25%, respectively [31]. In addition, the major emission sources of NO_x are land transport, waste incineration, and construction, with each accounting for more than 20%. The largest emission sources of CO were land transport, wastewater treatment, and organic solvents, while the major emission sources of sulfur oxides (SO_x) were waste incineration as well as commercial, domestic, and service industries [31]. The total estimated emissions of PM_{10} and $PM_{2.5}$ in 2021 will have decreased by 7.7% and 6.7%, respectively. A detailed breakdown is for PM_{10} and $PM_{2.5}$, respectively, is as follows, land transport decreased by 0.3% and 9.6%, maritime transport decreased by 18.5% and 18.5%, air transport increased by 8.7% and 8.7%, commercial, domestic and service industries increased by 3.5% and 3.6%, construction increased by 18.1% and 18.1%,

the industrial sector increased by 28.4% and 28.4%, local production of electricity decreased by 69.4% and 67.6%, and waste incineration increased by 1.6% and decreased by 0.1% respectively [31].

Nevertheless, the emission of PM_{10} on the road is often associated with road dust and particle emissions from brake pad wear [32,33]. In contrast, the emission of $PM_{2.5}$ on the road is often associated with the tailpipe emission of fossil-fuel-powered motor vehicles, and the switch to battery electric vehicles (BEVs) is an ideal measure to reduce the emission of $PM_{2.5}$ [34,35].

3.1. Observation Results

The levels of PM_{10} and $PM_{2.5}$ concentrations were collected in each of the four roadside locations, including Av. do Coronol Mesquita (S1), R. do Campo (S2-A and S2-B), R. da Ribeira do Patane (S3-A and S3-B), and Av. de Almeida Ribeiro (S4-A and S4-B). Each location consists of 48 non-consecutive hours of monitoring.

Table 2 shows the obtained average and standard deviation (SD) of PM_{10} and $PM_{2.5}$ on traffic-related sites in $\mu\text{g}/\text{m}^3$. The roadside location with the highest average of PM_{10} and $PM_{2.5}$ is recorded at Av. do Almeida, Ribeiro, with $40.8 \mu\text{g}/\text{m}^3$ and $19.2 \mu\text{g}/\text{m}^3$, respectively, while the lowest average of PM_{10} and $PM_{2.5}$ is recorded at Av. do Coronol Mesquita, with $38.4 \mu\text{g}/\text{m}^3$ and $18.1 \mu\text{g}/\text{m}^3$, respectively (see Table 2).

Table 2. Obtained average and standard deviation (SD) of PM_{10} and $PM_{2.5}$ on traffic-related sites, in $\mu\text{g}/\text{m}^3$ (Raw Data and Calibrated Data).

Site	PM_{10} (Raw Data)	$PM_{2.5}$ (Raw Data)	PM_{10} (Calibrated)	$PM_{2.5}$ (Calibrated)
Av. do Almeida Ribeiro	69.1 ± 25.9	66.3 ± 33.5	40.8 ± 15.6	19.2 ± 9.8
R. do Campo	67.5 ± 33.1	63.5 ± 30.0	39.8 ± 19.4	18.4 ± 8.7
R. da Ribeira do Patane	68.1 ± 30.6	66.0 ± 36.2	40.2 ± 18.2	19.1 ± 10.5
Av. do Coronol Mesquita	65.1 ± 28.5	62.5 ± 32.1	38.4 ± 16.8	18.1 ± 9.2

3.2. Distribution Analysis

Figure 6a shows the boxplot of PM_{10} average distribution by traffic site, including the first quartile, average (represented by x), median (represented by -), third quartile, and outliers (represented by dots). For Av. do Coronol Mesquita, the average is $38.4 \mu\text{g}/\text{m}^3$ and the median is $39.2 \mu\text{g}/\text{m}^3$. For R. do Campo, the average is $39.8 \mu\text{g}/\text{m}^3$ and the median is $36.0 \mu\text{g}/\text{m}^3$. For R. do Ribeira do Patane, the average is $40.2 \mu\text{g}/\text{m}^3$ and the median is $39.8 \mu\text{g}/\text{m}^3$. For Av. de Almeida Ribeiro, the average is $40.8 \mu\text{g}/\text{m}^3$ and the median is $40.4 \mu\text{g}/\text{m}^3$. Overall, the average and median values for PM_{10} mean distribution are within a close range for all four locations (Figure 6a).

Figure 6b shows the boxplot of $PM_{2.5}$ average distribution by traffic site, including the first quartile, average (represented by x), median (represented by -), third quartile, and outliers (represented by dots). For Av. do Coronol Mesquita, the average is $18.1 \mu\text{g}/\text{m}^3$ and the median is $16.0 \mu\text{g}/\text{m}^3$. For R. do Campo, the average is $18.4 \mu\text{g}/\text{m}^3$ and the median is $16.4 \mu\text{g}/\text{m}^3$. For R. do Ribeira do Patane, the average is $19.1 \mu\text{g}/\text{m}^3$ and the median is $15.7 \mu\text{g}/\text{m}^3$. For Av. de Almeida Ribeiro, the average is $19.2 \mu\text{g}/\text{m}^3$ and the median is $18.1 \mu\text{g}/\text{m}^3$. Overall, the average and median values for $PM_{2.5}$ mean distribution are within a close range for all four locations (Figure 6b).

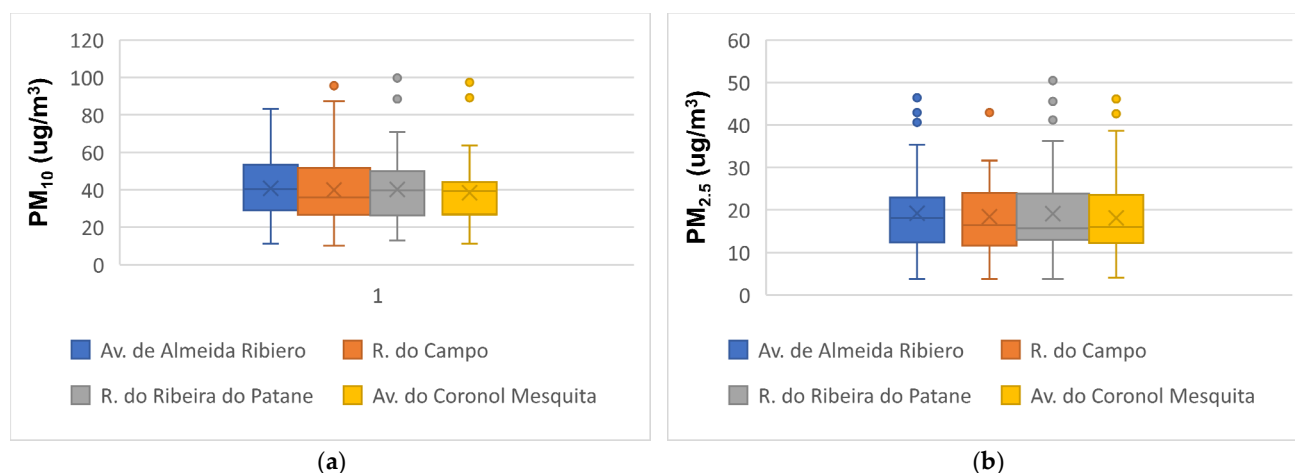


Figure 6. Boxplot of 1-min (a) PM_{10} and (b) $PM_{2.5}$ average distribution by traffic site (first quartile, average (x), median (-), third quartile, and outliers (dots)).

3.3. Traffic Characterization

Figure 7a shows the traffic characterization by type of vehicles in Av. do Coronol Mesquita over two sampling periods. The most popular type of vehicle is the motorcycle (48%), while the least popular type of vehicle is the heavy-duty vehicle (2%). Figure 7b shows the traffic characterization by type of vehicles in R. do Campo over two sampling periods. The most popular type of vehicle is the motorcycle (40%), while the least popular type of vehicle is the heavy-duty vehicle (2%). Figure 7c shows the traffic characterization by type of vehicle in R. da Ribeira do Patane over two sampling periods. The most popular type of vehicle is the motorcycle (56%), while the least popular type of vehicle is the heavy-duty vehicle (5%) and taxi (5%). Figure 7d shows the traffic characterization by type of vehicle in Av. de Almeida Ribeiro over two sampling periods. The most popular type of vehicle is the motorcycle (42%), while the least popular type of vehicle is the heavy-duty vehicle (3%) (Figure 7a–d).

Table 3 shows the average traffic flow in each sampling location per hour. Av. do Coronol Mesquita has the highest traffic flow, with 370 vehicles per hour, while Av. de Almeida Ribeiro has the lowest traffic flow, with 110 vehicles per hour (see Table 3).

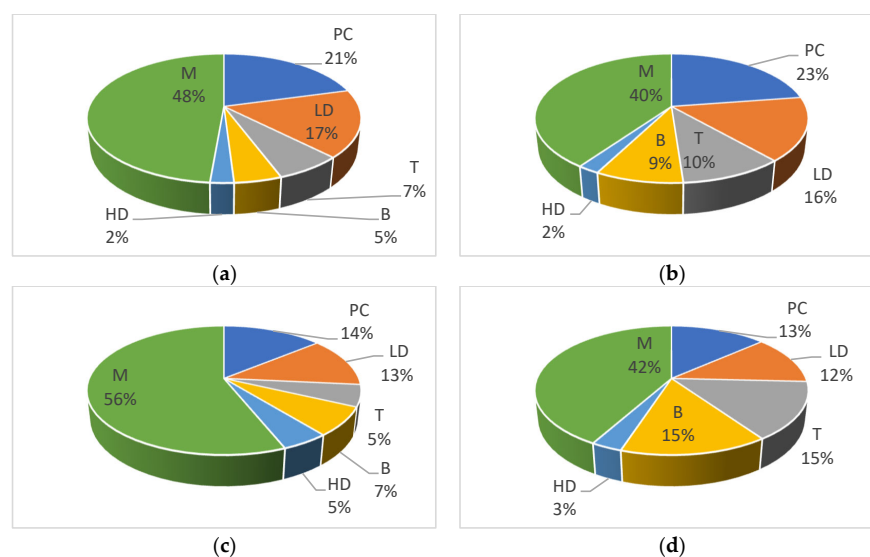


Figure 7. Traffic characterization by type of vehicle in (a) Av. do Coronol Mesquita, (b) R. do Campo, (c) R. da Ribeira do Patane, and (d) Av. de Almeida Ribeiro over two sampling periods. (PC—passenger cars; LD—light-duty vehicles; T—taxis; B—buses; HD—heavy-duty vehicles; M—motorcycles).

Table 3. Number of average traffic flow in each sampling location per hour.

Av. do Coronol Mesquita	370 vehicles
R. do Campo	190 vehicles
R. da Ribeira do Patane	180 vehicles
Av. de Almeida Ribeiro	110 vehicles

Table 4 shows the traffic characterization by Euro Emission Standard and types of vehicles in Av. do Coronol Mesquita, R. do Campo, R. da Ribeira do Patane, and Av. de Almeida Ribeiro, with vehicles characterized by different Euro Emission Standards and different types observed at each of the collection points and converted and presented in percentage as listed below (see Table 4).

Table 4. Traffic characterization by Euro Emission Standard and type of vehicle in Av. do Coronol Mesquita., R. do Campo., R. da Ribeira do Patane., and Av. de Almeida Ribeiro. (PC—passenger cars; LD—light-duty vehicles; T—taxis; B—buses; HD—heavy-duty vehicles; M—motorcycles).

Av. do Coronol Mesquita	PC	LD	T	B	HD	M
Euro 1	0%	0%	0%	0%	0%	0%
Euro 2	0%	0%	0%	1%	2%	0%
Euro 3	4%	2%	0%	4%	9%	1%
Euro 4	14%	10%	0%	4%	17%	3%
Euro 5	28%	27%	0%	34%	16%	25%
Euro 6	54%	61%	100%	57%	56%	71%
R. do Campo	PC	LD	T	B	HD	M
Euro 1	0%	0%	0%	0%	2%	0%
Euro 2	0%	0%	0%	0%	4%	0%
Euro 3	4%	2%	0%	0%	7%	1%
Euro 4	15%	10%	0%	5%	18%	4%
Euro 5	28%	26%	0%	39%	13%	26%
Euro 6	53%	62%	100%	56%	56%	69%
R. da Ribeira do Patane	PC	LD	T	B	HD	M
Euro 1	0%	0%	0%	0%	1%	0%
Euro 2	0%	0%	0%	0%	2%	0%
Euro 3	3%	2%	0%	1%	11%	1%
Euro 4	15%	12%	0%	4%	16%	4%
Euro 5	28%	26%	0%	30%	16%	26%
Euro 6	54%	60%	100%	65%	54%	69%
Av. de Almeida Ribeiro	PC	LD	T	B	HD	M
Euro 1	0%	0%	0%	0%	1%	0%
Euro 2	0%	0%	0%	0%	3%	0%
Euro 3	4%	2%	0%	0%	9%	0%
Euro 4	15%	11%	0%	5%	17%	5%
Euro 5	29%	26%	0%	30%	14%	24%
Euro 6	52%	61%	100%	65%	56%	71%

In Av. do Coronol Mesquita, the most popular type of emission standard is Euro 6, with 54% for the private car, 61% for the light-duty vehicle, 100% for the taxi, 57% for the bus, 56% for the heavy-duty vehicle, and 71% for the motorcycle. In R. do Campo, the most popular type of emission standard is Euro 6, with 53% for the private car, 62% for the light-duty vehicle, 100% for the taxi, 56% for the bus, 56% for the heavy-duty vehicle, and 69% for the motorcycle. In R. da Ribeira do Patane, the most popular type of emission standard is Euro 6, with 54% for the private car, 60% for the light-duty vehicle, 100% for the taxi, 65% for the bus, 54% for the heavy-duty vehicle, and 69% for the motorcycle. In Av. de Almeida Ribeiro, the most popular type of emission standard is Euro 6, with 52%

for the private car, 61% for the light-duty vehicle, 100% for the taxi, 65% for the bus, 56% for the heavy-duty vehicle, and 71% for the motorcycle. With the majority of the vehicles observed at the four roadside locations in Macao complying with EU 6 emission standards, it is expected that roadside emissions will continue to improve in Macao.

3.4. Correlation between Observed PM Concentration and the Number of Vehicles

Table 5 shows the statistical output for MLR analysis with a 95% confidence level between PM₁₀ and PM_{2.5} 1-h averages and the number of vehicles (hourly traffic flow). The result shows a weak relationship between the number of vehicles and the level of PM₁₀ concentration, with a correlation of determination (R^2) of ($R^2 = 0.001$ to 0.024). The result also shows a weak relationship between the number of vehicles and the level of PM_{2.5} concentration ($R^2 = 0.015$ to 0.122). The result shows that the traffic flow has an insignificant contribution to the concentration of PM₁₀ and PM_{2.5} in the monitored locations (see Table 5).

$$R^2 = 1 - \frac{\sum_{i=1}^n (y_{pred}^i - y_{true}^i)^2}{\sum_{i=1}^n (y_{true}^i - y_{average})^2} \quad (3)$$

$$p\text{-Value} = 1 - \text{Probability (Z-score)}. \quad (4)$$

In order to test the null hypothesis and alternative hypothesis below, the significance level is set at 0.05 to validate this hypothesis. The p -Value is shown in Table 5 (see Table 5).

Null Hypothesis (H0): *There is no relationship between PM concentrations and hourly traffic flow in the monitored locations in Macao.*

Alternate Hypothesis (H1): *There is a relationship between PM concentrations and hourly traffic flow in the monitored locations in Macao.*

Table 5. Coefficient of Determination and p -Value between PM concentration and hourly traffic flow.

Locations	PM ₁₀	PM _{2.5}		
	R^2	p -Value	R^2	p -Value
Av. de Almeida Ribeiro	0.005	0.623	0.076	0.059
R. do Campo	0.020	0.341	0.015	0.412
R. da Ribeira do Patane	0.024	0.289	0.036	0.194
Av. Do Coronol Mesquita	0.001	0.860	0.122	0.015

The result shows since the p -Value of all monitored locations except Av. Do Coronol Mesquita exceed the significance level, we failed to reject the null hypothesis. Thus, no relationship between the PM concentrations and hourly traffic flow can be established in this study.

3.5. Correlation between Observed PM Concentration and Traffic Characterization

Table 6 shows the statistical output for MLR analysis with a 95% confidence level between PM₁₀ and PM_{2.5} 1-h averages and the types of vehicles. The result shows a weak relationship between the types of vehicles and the level of PM₁₀ concentration, with a correlation of determination (R^2) of ($R^2 = 0.000$ to 0.007). The result also shows a weak relationship between the types of vehicles and the level of PM_{2.5} concentration ($R^2 = 0.001$ to 0.043). The result shows that the vehicle types have an insignificant contribution to the concentration of PM₁₀ and PM_{2.5} in the monitored locations (see Table 6).

Table 6. Coefficient of Determination and *p*-Value between PM concentration and type of vehicle.

Vehicle Types	PM ₁₀	PM _{2.5}		
	R ²	<i>p</i> -Value	R ²	<i>p</i> -Value
PC	0.001	0.643	0.001	0.646
LD	0.001	0.686	0.009	0.186
T	0.005	0.329	0.004	0.347
B	0.001	0.599	0.002	0.507
HD	0.000	0.835	0.043	0.004
M	0.007	0.247	0.021	0.044

In order to test the null hypothesis and alternative hypothesis below, the significance level is set at 0.05 to validate this hypothesis. The *p*-Value is shown in Table 6 (see Table 6).

Null Hypothesis (H0): *There is no relationship between PM concentrations and the types of vehicles in the monitored locations of Macao.*

Alternate Hypothesis (H1): *There is a relationship between PM concentrations and the types of vehicles in the monitored locations of Macao.*

The result show that since the *p*-Values of all vehicle types except HD and M for PM_{2.5} exceed the significance level, we failed to reject the null hypothesis. Thus, no relationship between PM concentrations and vehicle types can be established in this study. In addition, a similar study conducted in Brisbane, Australia, showed that there was a weak linear relationship between the total traffic volume and the roadside particle concentration [36]. Moreover, another study in Portland, Oregon, USA, showed that local traffic has no relationship with roadside PM_{2.5} concentrations [37]. In addition, a study in Shanghai, China, showed a weak linear relationship between total traffic volume and roadside PM_{2.5} concentrations [38]. Previous studies showed a similar result compared to the study conducted in Macao, which further ensures the robustness and quality of this study. It is not surprising to see that traffic flow and vehicle types have no significant contribution to the levels of PM₁₀ and PM_{2.5} concentrations because PM is generally known to be a regional problem caused by transboundary pollutants rather than a local emission problem.

4. Conclusions

According to The United Nations World Prospects Report, Macao was ranked as the world's most densely populated region [39]. It is very important to evaluate the roadside air quality in Macao. The present work aimed to evaluate the impact of road transportation on the levels of PM₁₀ and PM_{2.5} concentrations and to fulfill the lack of monitoring at several important roadside locations in Macao. Although the TSI Sidepak Monitor is simple and reliable equipment, it is necessary to calibrate it against the US EPA equivalent reference method to ensure the data reported is accurate. The calibration results show a correlation coefficient (*r*) of 0.79 between the field-calibrated equipment and the EPA equivalent reference method. The highest PM₁₀ and PM_{2.5} averages are recorded at Av. do Almeida, Ribeiro, with 40.8 µg/m³ and 19.2 µg/m³, respectively. The lowest PM₁₀ and PM_{2.5} averages are recorded at Av. do Coronol Mesquita, with 38.4 µg/m³ and 18.1 µg/m³, respectively. The traffic characterization provides an important perspective on the vehicle types that currently travel on the road in Macao. The result shows that the most popular type of vehicle in Macao is the motorcycle (>40%), while the least popular type of vehicle in Macao is the heavy-duty vehicle (<5%), during the monitoring campaign at the four roadside locations. The majority of private cars (>50%) on the road in Macao comply with the EU 6 emission standard. In addition, there is a weak relationship between the observed

PM₁₀ and PM_{2.5} concentrations and the hourly traffic flow ($R^2 = 0.001$ to 0.122). Moreover, there is a weak relationship between the observed PM₁₀ and PM_{2.5} concentrations and the vehicle types ($R^2 = 0.000$ to 0.043).

This result could be explained by the primary roadside pollutants being CO and NO_x instead of PM₁₀ and PM_{2.5}, as mentioned by the DSPA report [31], and the high levels of PM₁₀ and PM_{2.5} concentrations being a regional problem caused by transboundary pollutants brought by the northern monsoon from inland, as shown in Figure 1 [40,41]. As shown, there is little to no relationship between local traffic volume and roadside PM concentration in the monitored locations of Macao, leading us to conclude that PM concentration is more likely tied to regional sources and meteorological conditions. Nevertheless, the complex geographical setting of Macao is also likely an influential factor in this study. Future studies may consider exploring the presence of heavy metals in the roadside and residential areas of Macao [42,43]. The limitation of this study may include the PM measured being influenced by external factors presented in the environment, such as the smoking cigarettes from walking pedestrians and the exhaust fan from a nearby restaurant's kitchen.

Author Contributions: Conceptualization, T.M.T.L.; methodology, T.M.T.L.; software, T.M.T.L. and M.F.C.M.; validation, T.M.T.L. and M.F.C.M.; data curation, T.M.T.L. and M.F.C.M.; writing—original draft preparation, T.M.T.L. and M.F.C.M.; writing—review and editing, T.M.T.L.; supervision, T.M.T.L.; funding acquisition, T.M.T.L. All authors have read and agreed to the published version of the manuscript.

Funding: This research received no external funding.

Data Availability Statement: Third party data. Restrictions apply to the availability of these data.

Acknowledgments: The work developed was supported by the Macao Meteorological and Geophysical Bureau (SMG).

Conflicts of Interest: The authors declare no conflict of interest.

References

1. Lei, T.M.T.; Siu, S.W.I.; Monjardino, J.; Mendes, L.; Ferreira, F. Using Machine Learning Methods to Forecast Air Quality: A Case Study in Macao. *Atmosphere* **2022**, *13*, 1412. [\[CrossRef\]](#)
2. WHO. *World Health Statistics 2021: Monitoring Health for the SDGs, Sustainable Development Goals*; WHO: Geneva, Switzerland, 2021.
3. Zaheer, J.; Jeon, J.; Lee, S.-B.; Kim, J.S. Effect of Particulate Matter on Human Health, Prevention, and Imaging Using PET or SPECT. *Prog. Med. Phys.* **2018**, *29*, 81. [\[CrossRef\]](#)
4. Lei, M.T.; Monjardino, J.; Mendes, L.; Gonçalves, D.; Ferreira, F. Statistical Forecast of Pollution Episodes in Macao during National Holiday and COVID-19. *Int. J. Environ. Res. Public Health* **2020**, *17*, 5124. [\[CrossRef\]](#)
5. Song, S.; Wu, Y.; Zheng, X.; Wang, Z.; Yang, L.; Li, J.; Hao, J. Chemical Characterization of Roadside PM_{2.5} and Black Carbon in Macao during a Summer Campaign. *Atmos. Pollut. Res.* **2014**, *5*, 381–387. [\[CrossRef\]](#)
6. Taheri, A.; Aliasghari, P.; Hosseini, V. Black Carbon and PM_{2.5} Monitoring Campaign on the Roadside and Residential Urban Background Sites in the City of Tehran. *Atmos. Environ.* **2019**, *218*, 116928. [\[CrossRef\]](#)
7. Ropkins, K.; Beebe, J.; Li, H.; Daham, B.; Tate, J.; Bell, M.; Andrews, G. Real-World Vehicle Exhaust Emissions Monitoring: Review and Critical Discussion. *Crit. Rev. Environ. Sci. Technol.* **2009**, *39*, 79–152. [\[CrossRef\]](#)
8. Roh, M.; Jeon, S.; Kim, S.; Yu, S.; Heshmati, A.; Kim, S. Modeling Air Pollutant Emissions in the Provincial Level Road Transportation Sector in Korea: A Case Study of the Zero-Emission Vehicle Subsidy. *Energies* **2020**, *13*, 3999. [\[CrossRef\]](#)
9. Guang, W.; Li, L.J.; Xiang, R.B. PM_{2.5} and Its Ionic Components at a Roadside Site in Wuhan, China. *Atmos. Pollut. Res.* **2019**, *10*, 162–167. [\[CrossRef\]](#)
10. Wong, Y.K.; Huang, X.H.H.; Cheng, Y.Y.; Louie, P.K.K.; Yu, A.L.C.; Tang, A.W.Y.; Chan, D.H.L.; Yu, J.Z. Estimating Contributions of Vehicular Emissions to PM_{2.5} in a Roadside Environment: A Multiple Approach Study. *Sci. Total Environ.* **2019**, *672*, 776–788. [\[CrossRef\]](#)
11. Lee, S.C.; Cheng, Y.; Ho, K.F.; Cao, J.J.; Louie, P.K.K.; Chow, J.C.; Watson, J.G. PM_{1.0} and PM_{2.5} Characteristics in the Roadside Environment of Hong Kong. *Aerosol Sci. Technol.* **2006**, *40*, 157–165. [\[CrossRef\]](#)
12. Phanukarn, P.; Garivait, H.; Chinwetkitvanich, S. Black Carbon in PM_{2.5} at Roadside Site in Bangkok, Thailand. *Int. J. GEOMATE* **2020**, *19*, 81–87. [\[CrossRef\]](#)
13. Tang, V.T.; Oanh, N.T.K.; Rene, E.R.; Binh, T.N. Analysis of Roadside Air Pollutant Concentrations and Potential Health Risk of Exposure in Hanoi, Vietnam. *J. Environ. Sci. Health A Toxic Hazard. Subst. Environ. Eng.* **2020**, *55*, 975–988. [\[CrossRef\]](#)

14. Ginzburg, H.; Liu, X.; Baker, M.; Shreeve, R.; Jayanty, R.K.M.; Campbell, D.; Zielinska, B. Monitoring Study of the Near-Road PM_{2.5} Concentrations in Maryland. *J. Air Waste Manag. Assoc.* **2015**, *65*, 1062–1071. [\[CrossRef\]](#)
15. Cao, J.J.; Lee, S.C.; Ho, K.F.; Fung, K.; Chow, J.C.; Watson, J.G. Characterization of Roadside Fine Particulate Carbon and Its Eight Fractions in Hong Kong. *Aerosol Air Qual. Res.* **2006**, *6*, 106–122. [\[CrossRef\]](#)
16. Moutinho, J.L.; Liang, D.; Golan, R.; Sarnat, S.E.; Weber, R.; Sarnat, J.A.; Russell, A.G. Near-Road Vehicle Emissions Air Quality Monitoring for Exposure Modeling. *Atmos. Environ.* **2020**, *224*, 117318. [\[CrossRef\]](#) [\[PubMed\]](#)
17. Suroto, A.; Yusof, N.F.F.M.; Norfazlinda, W.; Ramli, N.A.; Shith, S. Influence of Outdoor Source on The Variations of Indoor PM_{2.5} Concentration and Its Morphological Properties in Roadside School Environment. *Int. J. Integr. Eng.* **2019**, *11*, 119–128. [\[CrossRef\]](#)
18. Kortoçi, P.; Motlagh, N.H.; Zaidan, M.A.; Fung, P.L.; Varjonen, S.; Rebeiro-Hargrave, A.; Niemi, J.V.; Nurmi, P.; Hussein, T.; Petäjä, T.; et al. Air Pollution Exposure Monitoring Using Portable Low-Cost Air Quality Sensors. *Smart Health* **2022**, *23*, 100241. [\[CrossRef\]](#)
19. Wadlow, I.; Paton-Walsh, C.; Forehead, H.; Perez, P.; Amirghasemi, M.; Guérette, E.A.; Gendek, O.; Kumar, P. Understanding Spatial Variability of Air Quality in Sydney: Part 2-a Roadside Case Study. *Atmosphere* **2019**, *10*, 217. [\[CrossRef\]](#)
20. Pope, F.D.; Gatari, M.; Ng'ang'a, D.; Poynter, A.; Blake, R. Airborne Particulate Matter Monitoring in Kenya Using Calibrated Low-Cost Sensors. *Atmos. Chem. Phys.* **2018**, *18*, 15403–15418. [\[CrossRef\]](#)
21. Yi, E.E.P.N.; Nway, N.C.; Aung, W.Y.; Thant, Z.; Wai, T.H.; Hlaing, K.K.; Maung, C.; Yagishita, M.; Ishigaki, Y.; Win-Shwe, T.T.; et al. Preliminary Monitoring of Concentration of Particulate Matter (PM_{2.5}) in Seven Townships of Yangon City, Myanmar. *Environ. Health Prev. Med.* **2018**, *23*, 53. [\[CrossRef\]](#)
22. Suleiman, A.; Tight, M.R.; Quinn, A.D. Assessment and Prediction of the Impact of Road Transport on Ambient Concentrations of Particulate Matter PM₁₀. *Transp. Res. D Transp. Environ.* **2016**, *49*, 301–312. [\[CrossRef\]](#)
23. Baca-López, K.; Fresno, C.; Espinal-Enríquez, J.; Martínez-García, M.; Camacho-López, M.A.; Flores-Merino, M.V.; Hernández-Lemus, E. Spatio-Temporal Representativeness of Air Quality Monitoring Stations in Mexico City: Implications for Public Health. *Front. Public Health* **2021**, *8*, 536174. [\[CrossRef\]](#)
24. Lv, H.; Li, H.; Qiu, Z.; Zhang, F.; Song, J. Assessment of Pedestrian Exposure and Deposition of PM₁₀, PM_{2.5} and Ultrafine Particles at an Urban Roadside: A Case Study of Xi'an, China. *Atmos. Pollut. Res.* **2021**, *12*, 112–121. [\[CrossRef\]](#)
25. Lopes, M.; Russo, A.; Monjardino, J.; Gouveia, C.; Ferreira, F. Monitoring of Ultrafine Particles in the Surrounding Urban Area of a Civilian Airport. *Atmos. Pollut. Res.* **2019**, *10*, 1454–1463. [\[CrossRef\]](#)
26. Lopes, M.; Russo, A.; Gouveia, C.; Ferreira, F. Monitoring of Ultrafine Particles in the Surrounding Urban Area of In-Land Passenger Ferries. *J. Environ. Prot.* **2019**, *10*, 838–860. [\[CrossRef\]](#)
27. Hong, S.; Yoo, H.; Cho, J.; Yeon, G.; Kim, I. Characteristics of Resuspended Road Dust with Traffic and Atmospheric Environment in South Korea. *Atmosphere* **2022**, *13*, 1215. [\[CrossRef\]](#)
28. Lei, M.T.; Monjardino, J.; Mendes, L.; Gonçalves, D.; Ferreira, F. Macao Air Quality Forecast Using Statistical Methods. *Air Qual. Atmos. Health* **2019**, *12*, 1049–1057. [\[CrossRef\]](#)
29. Shi, Y.; Ng, E. Fine-Scale Spatial Variability of Pedestrian-Level Particulate Matters in Compact Urban Commercial Districts in Hong Kong. *Int. J. Environ. Res. Public Health* **2017**, *14*, 1008. [\[CrossRef\]](#)
30. Kane, F.; Abbate, J.; Landahl, E.C.; Potosnak, M.J. Monitoring Particulate Matter with Wearable Sensors and the Influence on Student Environmental Attitudes. *Sensors* **2022**, *22*, 1295. [\[CrossRef\]](#)
31. DSPA. Report on the State of the Environment of Macao 2021. 2022. Available online: https://www.dspa.gov.mo/Publications/StateReport/2021/2021_en.pdf (accessed on 1 June 2023).
32. Mamakos, A.; Arndt, M.; Hesse, D.; Augsburg, K. Physical Characterization of Brake-Wear Particles in a PM₁₀ Dilution Tunnel. *Atmosphere* **2019**, *10*, 639. [\[CrossRef\]](#)
33. Casotti Rienda, I.; Alves, C.A.; Nunes, T.; Soares, M.; Amato, F.; Sánchez de la Campa, A.; Kováts, N.; Hubai, K.; Teke, G. PM₁₀ Resuspension of Road Dust in Different Types of Parking Lots: Emissions, Chemical Characterisation and Ecotoxicity. *Atmosphere* **2023**, *14*, 305. [\[CrossRef\]](#)
34. Kazemzadeh, E.; Koengkan, M.; Fuinhas, J.A. Effect of Battery-Electric and Plug-In Hybrid Electric Vehicles on PM_{2.5} Emissions in 29 European Countries. *Sustainability* **2022**, *14*, 2188. [\[CrossRef\]](#)
35. Ma, C.; Madaniyazi, L.; Xie, Y. Impact of the Electric Vehicle Policies on Environment and Health in the Beijing–Tianjin–Hebei Region. *Int. J. Environ. Res. Public Health* **2021**, *18*, 623. [\[CrossRef\]](#) [\[PubMed\]](#)
36. Johnson, L.; Ferreira, L. Modelling particle emissions from traffic flows at a freeway in Brisbane, Australia. *Transp. Res. Part D Transp. Environ.* **2001**, *6*, 357–369. [\[CrossRef\]](#)
37. Kendrick, C.M.; Koonce, P.; George, L.A. Diurnal and seasonal variations of no, no₂ and PM_{2.5} mass as a function of traffic volumes alongside an urban arterial. *Atmos. Environ.* **2015**, *122*, 133–141. [\[CrossRef\]](#)
38. Wang, Z.; Zhong, S.; He, H.; Peng, Z.-R.; Cai, M. Fine-scale variations in PM_{2.5} and black carbon concentrations and corresponding influential factors at an urban road intersection. *Build. Environ.* **2018**, *141*, 215–225. [\[CrossRef\]](#)
39. Sheng, N.; Tang, U.W. Risk assessment of traffic-related air pollution in a world heritage city. *Int. J. Environ. Sci. Technol.* **2013**, *10*, 11–18. [\[CrossRef\]](#)
40. Li, X.; Lopes, D.; Mok, K.M.; Miranda, A.I.; Yuen, K.V.; Hoi, K.I. Development of a road traffic emission inventory with high spatial-temporal resolution in the world's most densely populated region-Macau. *Environ. Monit. Assess.* **2019**, *191*, 239. [\[CrossRef\]](#)

41. Lopes, D.; Ferreira, J.; Hoi, K.I.; Miranda, A.I.; Yuen, K.V.; Mok, K.M. Weather Research and Forecasting Model Simulations over the Pearl River Delta Region. *Air Qual. Atmos. Health* **2019**, *12*, 115–125. [[CrossRef](#)]
42. Gupta, V.; Bisht, L.; Arya, A.K.; Singh, A.P.; Gautam, S. Spatially Resolved Distribution, Sources, Exposure Levels, and Health Risks of Heavy Metals in <63 µm Size-Fractionated Road Dust from Lucknow City, North India. *Int. J. Environ. Res. Public Health* **2022**, *19*, 12898. [[CrossRef](#)]
43. Kumar, R.P.; Perumpully, S.J.; Samuel, C. Exposure and health: A progress update by evaluation and scientometric analysis. *Stoch. Environ. Res. Risk Assess.* **2023**, *37*, 453–465. [[CrossRef](#)] [[PubMed](#)]

Disclaimer/Publisher's Note: The statements, opinions and data contained in all publications are solely those of the individual author(s) and contributor(s) and not of MDPI and/or the editor(s). MDPI and/or the editor(s) disclaim responsibility for any injury to people or property resulting from any ideas, methods, instructions or products referred to in the content.